The use of bilayers consisting of graphene and noble metals has been explored for biosensors that employ inverted surface plasmon resonance

Chidi Yun [1], Miki Shun [1], Keypi Jackson [2], Ladson Newiduom [2], Ibrina Browndi [2]
[1] Department of Computer Science, Rivers State University, Port Harcourt, Nigeria
[2] Department of Urban and Regional Planning, Rivers State University, Port Harcourt, Nigeria

ABSTRACT

The article introduces biosensors based on inverted surface plasmon resonance (ISPR) technology, which utilize thin metal films that absorb light with a graphene layer on top. The researchers investigated two systems, one made of palladium/graphene and the other made of iridium/graphene, using numerical analysis. The study highlights the characteristics and abilities of these biosensors, which offer potential for precise, sensitive, and efficient detection of multiple biomolecular interactions. Inverted surface plasmon resonance (ISPR) biosensors based on absorbent metal thin films with a graphene sheet on top are presented. Two systems have been examined by means of a numerical study, a bilayer of palladium/graphene and one of iridium/graphene. The features and performances of such biosensors are discussed. The proposed ISPR systems potentially disclose new strategies for high-resolution, sensitive and straightforward detection of multiple biomolecular interactions.

KEYWORDS: large-eddy simulation, surface plasmon resonance, graphene, biosensors

1.0 INTRODUCTION

The article presents a novel type of biosensor known as an inverted surface plasmon resonance (ISPR) biosensor, which is made up of a metal thin film and a graphene layer on top. The study focuses on two specific systems: a palladium/graphene bilayer and an iridium/graphene bilayer, both of which were analyzed using numerical simulations. The article goes on to discuss the characteristics and capabilities of these biosensors, which have the potential to offer new approaches for highly sensitive and precise detection of multiple biomolecular interactions [1-11]. The main features of an effective biosensor are good sensitivity and resolution, high-quality signal, long-term stability, significant precision and selectivity, and regeneration after ligand binding. It is not easy to fulfil all of these requirements and a compromise is often achieved as a result of new technological developments and materials investigation. In surface plasmon resonance (SPR) biosensors, surface plasmon polaritons (SPP) are electromagnetic evanescent waves excited to probe the interactions between the biomolecules and the sensor metallic surface. The excitation is perpendicularly confined at the interface between the metal and the dielectric sensing medium and its propagation is affected by the local gradient of refractive index induced by changes in biomolecule concentrations and chemical reactions. These effects can be optically measured by the attenuated total reflection method. In fact, a minimum in the reflectivity occurs when the momentum of the incident light in the plane of the surface matches that of the SPP mode and no reflection appears. In the conventional Kretschmann configuration for a SPR biosensor, a thin metallic film is interposed between the sensing medium and one side of a prism. The metallic film is typically a noble metal that supports the propagation of SPP at visible light frequencies. Gold (Au) is usually preferred thanks to its good sensitivity and excellent resistance to oxidation and corrosion, but, unfortunately, it shows a broadened curve profile and lacks biomolecular affinity [12-19]. These issues limit the performance of conventional Au based SPR devices. Different solutions are under investigation to overcome the poor adsorption of biomolecules. A possible strategy is to use biomolecular recognition elements (BREs), such as nanoparticles, nanoholes and metallic nanoslits as adhesion, even though the fine control of the geometrical and optical properties of the nanostructure is itself a cutting edge research topic. Structures based on Au/graphene bilayers have been recently realized and characterized. Graphene both enhances the biomolecular affinity and possibly makes the device more resistant to contamination and oxidation processes. The full potential of graphene as a protection layer can be understood based on its unique physical and chemical properties. The physical

surface of sp2 carbon allotropes forms a natural diffusion barrier thus providing a physical separation between the protected metal and reactants. Thus, in principle, perfect graphene without defects and grain boundaries is able to preserve the surface of the metal under reactive environments over a long period of time [20-28]. Actually, real graphene shows a non-ideal behavior, defects and grain boundaries, but further advances in growth and transfer are expected to guarantee a high-quality large-domain single graphene layer (SGL). Concerning the natural broader signal of Au, it is a weak point that still persists. Silver (Ag) is often considered the alternative material to overcome this drawback because it shows a theoretical sharper curve, but, unfortunately, while on the one hand it allows better performances, on the other hand it is highly susceptible to oxidation, which greatly lowers its features. Eventually, while Au might be a better choice for stability and reliability, Ag should be a promising candidate for the sensitive SPR biosensor if its surface can be protected to become chemically inert. The idea of passivating the pristine Ag layer by means of graphene sheets has been investigated as well. The concept is tempting in perspective, but not yet reliable considering the actual state of the art. Recent results suggest that the grain boundaries of graphene are likely to be the main contributor to oxidation of the underlying metals. Unfortunately for high reactive materials such as Ag, the degradation process is inexorable and not confined. Moreover, previous studies found that silver oxide dramatically reduces the significant sensitivity of the silver substrate, so gold can be still assumed the basis for comparison. SPR devices are arranged by adopting different schemes. Depending on which modulation approach is used, the detector records the intensity of the light, its wavelength or angular spectrum. Whatever the interrogation scheme selected, other relevant parameters define the SPR biosensor performances, such as dynamic range, contrast, sharpness and signal to noise ratio. The dominant sources of noise are fluctuations of light intensity emitted by the light source, statistical properties of light and noise generated in the electronic circuitry of the detector. However, in any modulation scheme the output signals under the noise level cannot be precisely detected. The signal to noise ratio can be improved by acquiring more images and summing them, but this is not easy to achieve in the case of biomolecular dynamic detection. In fact, output signals higher than noise should be preferably required, otherwise part of the information could be lost. In this respect, a minimum signal against a noisy background can sometimes prove to be problematic, so if a sharp maximum reflectivity signal can be obtained the design of a practical sensing device may be more readily facilitated, and the accuracy and the resolution of the measurements improved. Many years ago the observation of a maximum in reflectivity coinciding with the excitation of SPP has been reported. The physical phenomena is known as inverted surface plasmon resonance (ISPR) and it has been investigated for different metals. The idea we propose is to exploit the features of noble metals with ISPR behavior for high-resolution biosensors development. In particular, iridium (Ir) and palladium (Pd) have been considered. Iridium is known for its inertness and robustness, while palladium is more sensitive and reactive. Last, but not least, we borrow the concept to improve the performances of such biosensors by using graphene as a BRE and capping layer, knowing well the limits imposed by real graphene growth. The first attempts to cap Pd and Ir with graphene sheets have already been tested. Results of our numerical study show that the structures proposed are valuable for high-resolution, sensitive and accurate ISPR imaging biosensors [29-35].

Meeting all of the requirements for biosensors can be challenging, and often compromises must be made through the use of new technologies and materials. Surface plasmon resonance (SPR) biosensors use surface plasmon polaritons (SPP), which are evanescent electromagnetic waves, to detect interactions between biomolecules and the metal surface of the sensor. These waves are confined perpendicularly at the interface between the metal and the sensing medium and their propagation is affected by changes in biomolecule concentrations and chemical reactions, which alter the local gradient of refractive index. Meeting all of the requirements in surface plasmon resonance (SPR) biosensors can be challenging, and a compromise is often necessary due to advancements in technology and material exploration. In these types of biosensors, surface plasmon polaritons (SPP) are utilized to investigate interactions between biomolecules and the sensor's metallic surface. This is achieved by exciting electromagnetic evanescent waves, which are confined perpendicularly at the interface between the metal and the dielectric sensing medium. The propagation of these waves is influenced by changes in biomolecule concentrations and chemical reactions, which create local gradients in refractive index [35-48].

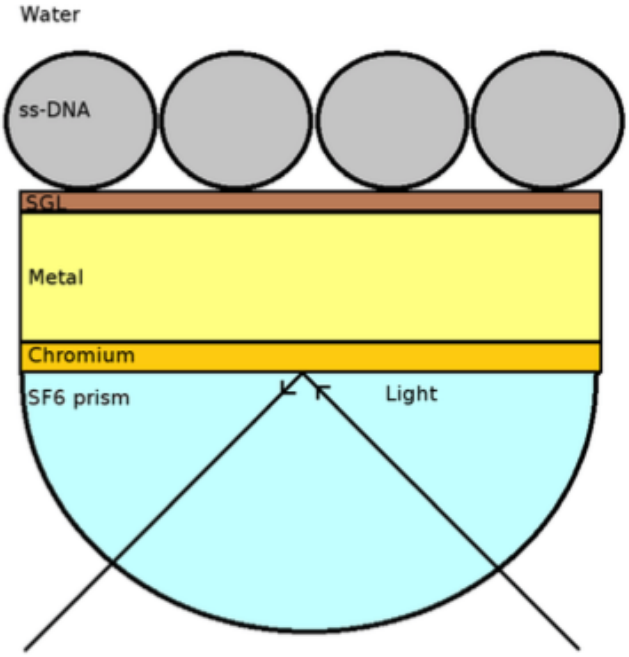

Figure 1. Schematic model of SPR biosensors based on a single graphene layer (SGL) and noble metals. A noble metal is deposited on a SF6 prism substrate with a chromium layer of 2 nm interposed. The SGL (0.34 nm) is on the top of the metal and acts as a biomolecular recognition element (BRE) as well as a protective layer.

2.0 BIOSENSORS DESIGN

The target chemical process of the performed analysis is the hybridization of (ss)-DNA during (ds)-DNA formation. The schematic model of the detector is shown in figure 1. It consists of a noble metal thin film deposited onto a SF6 cylindrical prism with 2 nm of chromium interposed for adhesion. A SGL covers the metallic surface, preserving, in the ideal case, the device from oxidation and contamination while acting as a BRE for DNA. Ir and Pd are the noble metals considered for samples SIr and SPd respectively, while a quasi-standard biosensor based on Au (SAu) has been used as a reference. Referring to the angular interrogation scheme, the layer thicknesses of the samples have been optimized to reach the best compromise between the peak shift due to variation of the medium's refractive index, the full-width at half-maximum (FWHM) of the signal, and the maximum contrast C of the signal: The chemical process being analyzed is the hybridization of (ss)-DNA during (ds)-DNA formation. Figure 1 shows a schematic model of the detector, which is composed of a noble metal thin film deposited onto a SF6 cylindrical prism. A layer of chromium (2 nm) is interposed for adhesion. The metallic surface is covered by a SGL, which serves as a BRE for DNA and ideally protects the device from oxidation and contamination. Samples SIr and SPd consist of Ir and Pd, respectively, while a standard biosensor based on Au (SAu) has been used as a reference. The layer thicknesses of the samples have been optimized to achieve the best compromise between the peak shift due to changes in the refractive index of the medium, the full-width at half-maximum (FWHM) of the signal, and the maximum contrast C of the signal, in reference to the angular interrogation scheme [1-17].

$$C = \frac{I_{\max} - I_{\min}}{I_{\max} + I_{\min}} \qquad (1)$$

($I_{\max/\min}$ are the maximum/minimum intensities of the detected reflectance).

Table 1. The structures proposed are Ir/SGL (S_{Ir}), Pd/SGL (S_{Pd}) and Au/SGL (S_{Au}), the last one as a reference. Thicknesses of the layers, real and imaginary parts of the refractive ($\tilde{n} = n + ik$) indices of the materials are reported together with the reference.

Materials	S_{Ir}	S_{Pd}	S_{Au}	n ($\lambda = 632.8$ nm)	k ($\lambda = 632.8$ nm)	Reference
SGL	0.34 nm	0.34 nm	0.34 nm	3.000	1.149	[24]
Ir	12.00 nm	—	—	2.528	4.613	[25]
Pd	—	14.00 nm	—	1.770	4.289	[26]
Au	—	—	50.00 nm	0.197	3.090	[25]
Cr	2.00 nm	2.00 nm	2.00 nm	3.135	3.310	[26]
SF6	Bulk	Bulk	Bulk	1.799	0.000	[27]

The desired signal is sharp and bright, indicating a high contrast and narrow FWHM. As previously highlighted, high contrast and narrow profile allow more precise investigations with higher signal to noise ratio. A quality factor Q can be thus defined starting from FWHM and C and assuming that a real signal exists (then FWHM and C are finite physical quantities):

$$Q \propto \frac{C}{\mathrm{FWHM}}. \quad (2)$$

In essence the quality factor Q describes how the signal approaches a Dirac delta function.

The sensitivity S is formally defined as S = dY B, where dn Y is the output signal, depending on the modulation mode, and B the molecular recognition coefficient, which we have assumed to be unitary. In the angular interrogation scheme the peak shift dp is the parameter to monitor, thus the sensitivity can be redefined as follows:

$$S = \frac{dp}{dn}. \quad (3)$$

Linear sensing in a wide dynamic range is furthermore desirable for biosensors used for quantitative monitoring interactions.

The thickness and the refractive index of the materials used for the proposed biosensors and for the reference sample SAu are summarized in table 1. Structures based on Au/graphene bilayers have been recently realized and characterized as SPR imaging biosensors.

Moreover, such biosensors have been conceived to detect the biomolecular reaction of single stranded (ss)-DNA and the consequent formation of double stranded (ds)-DNA. According to the state of the art, this process has been modeled as a 100 nm dielectric layer having the real part of the refractive index n varying from 1.462 to 1.480 during the double stranded (ds)-DNA formation. We assume to use a TM polarized He–Ne laser (λ0 = 632.8 nm) as a probe and the light propagation to occur along the z-axis of the devices. A Matlab code based on the transfer matrix method, valid for an optical structure consisting of N layers, has been used in order to obtain the reflectivity RTM of the ISPR biosensors proposed [18-36].

3.0 RESULTS AND DISCUSSION

Metals showing reflectivity maxima usually have high absorbance (|k| > |n|). We have investigated many absorbent materials in order to design the models proposed. Some of them are still under study and will probably be the subject of further investigations. In this analysis we have considered palladium and iridium, which have been chosen for their ISPR behavior and feasibility to deposit a graphene sheet on top. Palladium has already been used in surface plasmon resonance sensors, especially for hydrogen detection. Its good reactivity makes it particularly sensitive,

Table 2. Refractive index of the medium, contrast C, FWHM, angle and quality factor of the signal.

Structure	Refractive index n	Contrast	FWHM (deg)	Angle (deg)	Q (deg)$^{-1}$
S_{Ir}	1.332	0.999	2.701	48.015	0.369
	1.462	0.986	6.101	50.230	0.162
	1.480	0.982	6.729	50.640	0.146
S_{Pd}	1.332	0.993	3.043	48.105	0.326
	1.462	0.961	6.728	50.455	0.143
	1.480	0.954	7.328	50.880	0.130
S_{Au}	1.332	0.966	5.673	55.585	0.170
	1.462	0.928	8.184	64.340	0.113
	1.480	0.915	8.573	65.896	0.107

but on the other hand it affects its performances, leading to oxidation and contamination processes. Presently the problem can be partially solved by adding graphene as a capping layer, but with some misgivings, as for silver. In contrast, Ir has never been considered for SPR setups, even though it is inert and resistant to harsh environments. In any case, a SGL added to the pristine optimized designs can potentially help to protect the metal underneath and enhance the bioaffinity. In fact, it acts as an adhesion layer for DNA given that graphene adsorbs biomolecules with carbon based ring structures [37-48].

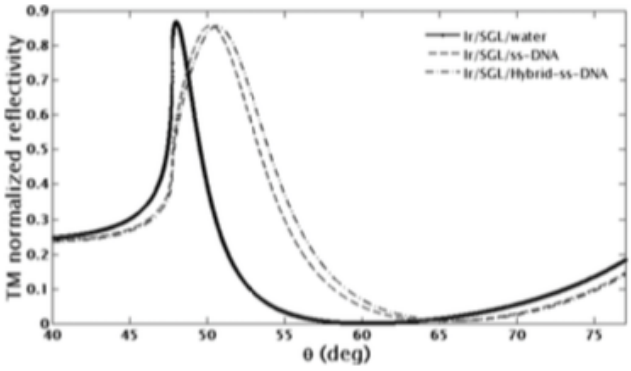

Figure 2. ISPR coupling features for S_{Ir} in water (black line) and during the DNA detection (dashed lines).

The plots hereafter show the optical response of the SIr (figure 2) and SPd (figure 3) systems, which have been compared with the reference biosensor based on Au SAu (figure 3, inset) in terms of peak shift, change of reflectivity profile and quality factor Q (equation (2)). Three different environments corresponding to three different steps of the detection have been analyzed: water (n = 1.332), (ss)-DNA (n = 1.462) and hybrid (ss)-DNA (n = 1.480). We have supposed to operate in an aqueous medium (figures 2 and 3, black lines) before the SGL catches the (ss)-DNA and detects its chemical changes (figures 2 and 3, dashed lines). From a qualitative point of view, all the metals show significant peak shifts and worsening of the profiles due the biomolecule capture, although the observed effects becomes less striking during the hybrid (ss)-DNA formation [15-29].

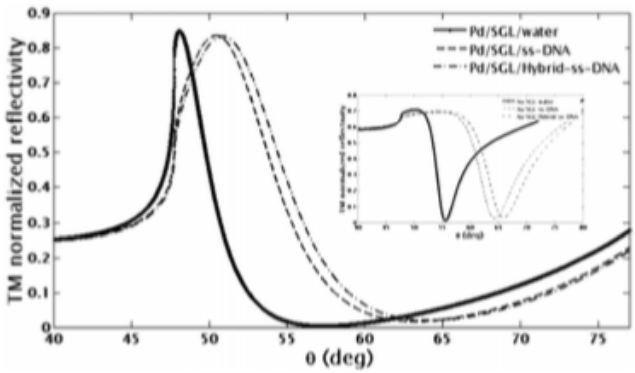

Figure 3. ISPR signal of the S_{Pd} biosensors in water (black line) and during the (ds)-DNA formation (dashed lines). We note that the peak shift is still appreciable for the two states of DNA.

Table 2 summarizes the quantitative analysis of the structure proposed in terms of contrast C,FWHM and detection angle at fixed refractive index n. It is worth noticing that for all the metals dp changes linearly with the refractive index, as is shown in figure 4 for the Ir. This fact is very important because a close to linear sensing performance is required for quantitative monitoring of biomolecular interactions [29-38].

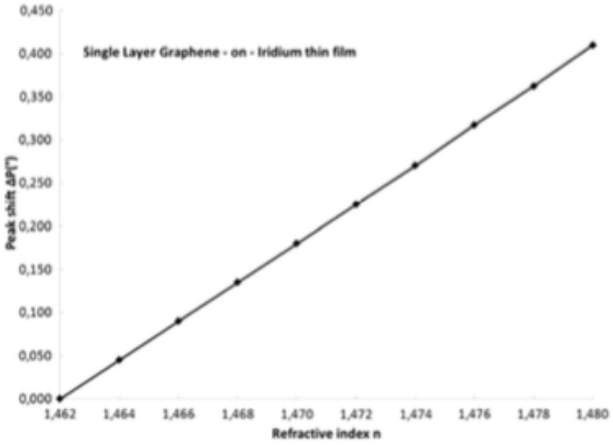

Figure 4. Sensitivity of the S_{Ir} SPR sensor during the ss-DNA hybridization.

The sensitivity of SAu is better than those of SIr and SPd. The peak shift associated with the (ds)-DNA formation is 1.560◦ in the case of SAu, 0.425◦ and 0.410◦ for SPd and SIr respectively (see table 2). However, the identification of the minimum itself depends on the noise level and the detection accuracy can thus be compromised and a maximum signal preferred. Moreover, if on one hand SAu allows for sensitivity advantages, on the other hand it shows a definitely broader signal profile than SIr and SPd (see figure 3 and table 2) with a lower contrast. From an operational point of view, it means better sensitivity but worse detection precision and resolution [39-48].

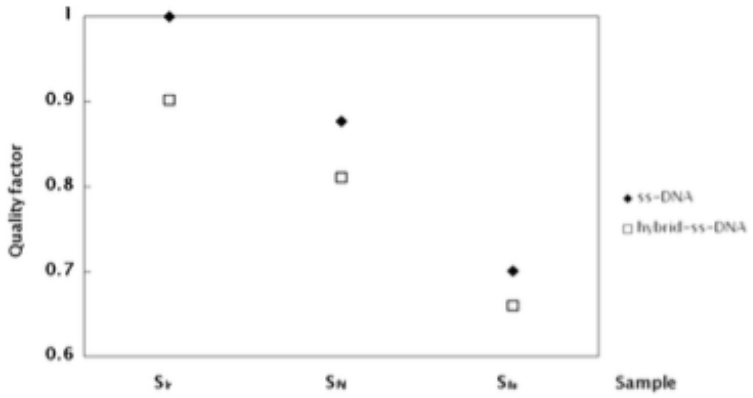

Figure 5. ISPR coupling features for S_{Ir} in water (black rhombus) and DNA reaction (empty squares). The quality factor Q for S_{Ir} is 27% higher than for S_{Au}.

The quality factors Q of the signals have been estimated for all the samples assuming the (ss)-DNA and hybrid (ss)-DNA as a medium; the corresponding value of the Q for SIr detecting (ss)-DNA has been used as the normalizing factor. The Q factor of SIr is always higher than SPd and SAu (figure 5): in the case of hybrid (ss)-DNA, it is 27% and 11% higher than for SAu and SPd respectively. These results highlighted that, in some aspects, the proposed structures are preferable to Au based biosensors. It does not mean that they are superior absolutely, but better for some applications, especially for process dynamic control. Therefore, the choice of the proper tool is not trivial and depends strictly on the target detection.

4.0 CONCLUSION

Two systems based respectively on the Pd/graphene and Ir/graphene structures have been conceived as inverted surface plasmon resonance biosensors for quantitative monitoring of biomolecule interactions and dynamics. They show some innovative aspects: a reflectivity maximum as the signal, an improved resistance to oxidation and contamination, and an estimated higher bioaffinity. In fact, the graphene layer can act as a biomolecular recognition element as well as a potential protective element. The characteristics of both devices have been analyzed in reference to a quasi-standard Au/graphene system. The results of the analysis claim better sensitivity for the Au based device, but a higher contrast and a sharper profile for the Ir and Pd based biosensors. These aspects must be considered as well in order to improve the overall signal to noise ratio. Furthermore, a maximum signal it easier to detect independently to the noise background. The SGL deposition development will hopefully allow high-quality single layer crystal graphene to be applied. Then, both Pd/graphene and the Ir/graphene bilayers should be proposed for accurate quantitative monitoring of biomolecular interactions, potentially opening new possibilities for innovative, high-resolution, sensitive and selective biosensors.

REFERENCES

[1] Rozhkov, Alexandr Vladimirovich, et al. "Electronic properties of graphene-based bilayer systems." Physics Reports 648 (2016): 1-104.
[2] Tang, Zuge, Behrad Zeinali, and Sarkew S. Abdulkareem. "Phase controlling of electromagnetically induced grating." Laser Physics Letters 19.5 (2022): 055204.
[3] Oostinga, Jeroen B., et al. "Gate-induced insulating state in bilayer graphene devices." Nature materials 7.2 (2008): 151-157.
[4] Zare, Saman, Behrad Zeinali Tajani, and Sheila Edalatpour. "Effect of nonlocal electrical conductivity on near-field radiative heat transfer between graphene sheets." Physical Review B 105.12 (2022): 125416.
[5] Oostinga, Jeroen B., et al. "Gate-induced insulating state in bilayer graphene devices." Nature materials 7.2 (2008): 151-157.
[6] Afroozeh, Abdolkarim, and Behrad Zeinali. "Improving the sensitivity of new passive optical fiber ring sensor based on meta-dielectric materials." Optical Fiber Technology 68 (2022): 102797.
[7] Xian, Lede, Salvador Barraza-Lopez, and M. Y. Chou. "Effects of electrostatic fields and charge doping on

the linear bands in twisted graphene bilayers." Physical Review B 84.7 (2011): 075425.
[8] Zeinali, Behrad, and Jafar Ghazanfarian. "Turbulent flow over partially superhydrophobic underwater structures: The case of flow over sphere and step." Ocean Engineering 195 (2020): 106688.
[9] Song, Zhida, et al. "All magic angles in twisted bilayer graphene are topological." Physical review letters 123.3 (2019): 036401.
[10] Zeinali, Behrad, Jafar Ghazanfarian, and Bamdad Lessani. "Janus surface concept for three-dimensional turbulent flows." Computers & Fluids 170 (2018): 213-221.
[11] Cao, Yuan, et al. "Tunable correlated states and spin-polarized phases in twisted bilayer–bilayer graphene." Nature 583.7815 (2020): 215-220.
[12] Zavareh, Bozorgasl, Hossein Foroozan, Meysam Gheisarnejad, and Mohammad-Hassan Khooban. "New trends on digital twin-based blockchain technology in zero-emission ship applications." Naval Engineers Journal 133, no. 3 (2021): 115-135.
[13] Li, J. I. A., et al. "Negative Coulomb drag in double bilayer graphene." Physical review letters 117.4 (2016): 046802.
[14] Bozorgasl, Zavareh, and Mohammad J. Dehghani. "2-D DOA estimation in wireless location system via sparse representation." In 2014 4th International Conference on Computer and Knowledge Engineering (ICCKE), pp. 86-89. IEEE, 2014.
[15] Huang, Shengqiang, et al. "Topologically protected helical states in minimally twisted bilayer graphene." Physical review letters 121.3 (2018): 037702.
[16] Piomelli, Ugo. "Large-eddy simulation: achievements and challenges." Progress in aerospace sciences 35.4 (1999): 335-362.
[17] Tang, Zhenhua, et al. "Graphene-based polymer bilayers with superior light-driven properties for remote construction of 3D structures." Advanced Science 4.5 (2017): 1600437.
[18] Sagaut, Pierre. Large eddy simulation for incompressible flows: an introduction. Springer Science & Business Media, 2006.
[19] Perali, Andrea, David Neilson, and Alex R. Hamilton. "High-temperature superfluidity in double-bilayer graphene." Physical review letters 110.14 (2013): 146803.
[20] Zhiyin, Yang. "Large-eddy simulation: Past, present and the future." Chinese journal of Aeronautics 28.1 (2015): 11-24.
[21] Poncharal, Philippe, et al. "Raman spectra of misoriented bilayer graphene." Physical Review B 78.11 (2008): 113407.
[22] Mason, Paul J. "Large-eddy simulation: A critical review of the technique." Quarterly Journal of the Royal Meteorological Society 120.515 (1994): 1-26.
[23] Lee, Dong Kyu, et al. "Graphene Oxide/Carbon Nanotube Bilayer Flexible Membrane for High-Performance Li–S Batteries with Superior Physical and Electrochemical Properties." Advanced Materials Interfaces 6.7 (2019): 1801992.
[24] Lesieur, Marcel, Olivier Métais, and Pierre Comte. Large-eddy simulations of turbulence. Cambridge university press, 2005.
[25] Xiao, B. B., et al. "Boosting oxygen reduction electrocatalysis of graphene-based bilayer heterojunction." Surfaces and Interfaces 33 (2022): 102232.
[26] Zalnejad, Kaveh, Seyyed Fazlollah Hossein, and Yousef Alipour. "The Impact of Livable City's Principles on Improving Satisfaction Level of Citizens; Case Study: District 4 of Region 4 of Tehran Municipality." Armanshahr Architecture & Urban Development 12.28 (2019): 171-183.
[27] Zalnezhad, Kaveh, Mahnaz Esteghamati, and Seyed Fazlollah Hoseini. "Examining the Role of Renovation in Reducing Crime and Increasing the Safety of Urban Decline Areas, Case Study: Tehran's 5th District." Armanshahr Architecture & Urban Development 9.16 (2016): 181-192.
[28] Motalo, Kubura, et al. "Hybrid nanostructures consisting of as-grown graphene and copper nanoparticles have been developed to improve the intensity and stability of surface plasmon resonance." International Journal of Basis Applied Science and Study 13.24 (2022): 2561-2570.
[29] Olutola, Tomiloba, et al. "A diffraction grating made of liquid crystals that can be controlled through electro-optic resources." International Journal of Management System and Applied Science 14.12 (2022): 42-51.
[30] Balen, John, et al. "Quantum plasmonic sensing is employed to experimentally measure kinetic parameters." Journal of Basis Applied Science and Management System 8.7 (2022): 136-146.
[31] Sharifani, Koosha and Amini, Mahyar and Akbari, Yaser and Aghajanzadeh Godarzi, Javad. "Operating Machine Learning across Natural Language Processing Techniques for Improvement of Fabricated News Model." International Journal of Science and Information System Research 12.9 (2022): 20-44.
[32] Amini, Mahyar, et al. "MAHAMGOSTAR.COM AS A CASE STUDY FOR ADOPTION OF LARAVEL FRAMEWORK AS THE BEST PROGRAMMING TOOLS FOR PHP BASED WEB DEVELOPMENT FOR SMALL AND MEDIUM ENTERPRISES." Journal of Innovation & Knowledge, ISSN (2021): 100-110.
[33] Amini, Mahyar, and Aryati Bakri. "Cloud computing adoption by SMEs in the Malaysia: A multi-perspective framework based on DOI theory and TOE framework." Journal of Information Technology & Information Systems Research (JITISR) 9.2 (2015): 121-135.

[34] Amini, Mahyar, and Nazli Sadat Safavi. "A Dynamic SLA Aware Heuristic Solution For IaaS Cloud Placement Problem Without Migration." International Journal of Computer Science and Information Technologies 6.11 (2014): 25-30.
[35] Amini, Mahyar. "The factors that influence on adoption of cloud computing for small and medium enterprises." (2014).
[36] Amini, Mahyar, et al. "Development of an instrument for assessing the impact of environmental context on adoption of cloud computing for small and medium enterprises." Australian Journal of Basic and Applied Sciences (AJBAS) 8.10 (2014): 129-135.
[37] Amini, Mahyar, et al. "The role of top manager behaviours on adoption of cloud computing for small and medium enterprises." Australian Journal of Basic and Applied Sciences (AJBAS) 8.1 (2014): 490-498.
[38] Amini, Mahyar, and Nazli Sadat Safavi. "A Dynamic SLA Aware Solution For IaaS Cloud Placement Problem Using Simulated Annealing." International Journal of Computer Science and Information Technologies 6.11 (2014): 52-57.
[39] Sadat Safavi, Nazli, Nor Hidayati Zakaria, and Mahyar Amini. "The risk analysis of system selection and business process re-engineering towards the success of enterprise resource planning project for small and medium enterprise." World Applied Sciences Journal (WASJ) 31.9 (2014): 1669-1676.
[40] Sadat Safavi, Nazli, Mahyar Amini, and Seyyed AmirAli Javadinia. "The determinant of adoption of enterprise resource planning for small and medium enterprises in Iran." International Journal of Advanced Research in IT and Engineering (IJARIE) 3.1 (2014): 1-8.
[41] Sadat Safavi, Nazli, et al. "An effective model for evaluating organizational risk and cost in ERP implementation by SME." IOSR Journal of Business and Management (IOSR-JBM) 10.6 (2013): 70-75.
[42] Safavi, Nazli Sadat, et al. "An effective model for evaluating organizational risk and cost in ERP implementation by SME." IOSR Journal of Business and Management (IOSR-JBM) 10.6 (2013): 61-66.
[43] Amini, Mahyar, and Nazli Sadat Safavi. "Critical success factors for ERP implementation." International Journal of Information Technology & Information Systems 5.15 (2013): 1-23.
[44] Amini, Mahyar, et al. "Agricultural development in IRAN base on cloud computing theory." International Journal of Engineering Research & Technology (IJERT) 2.6 (2013): 796-801.
[45] Amini, Mahyar, et al. "Types of cloud computing (public and private) that transform the organization more effectively." International Journal of Engineering Research & Technology (IJERT) 2.5 (2013): 1263-1269.
[46] Amini, Mahyar, and Nazli Sadat Safavi. "Cloud Computing Transform the Way of IT Delivers Services to the Organizations." International Journal of Innovation & Management Science Research 1.61 (2013): 1-5.
[47] Abdollahzadegan, A., Che Hussin, A. R., Moshfegh Gohary, M., & Amini, M. (2013). The organizational critical success factors for adopting cloud computing in SMEs. Journal of Information Systems Research and Innovation (JISRI), 4(1), 67-74.
[48] Khoshraftar, Alireza, et al. "Improving The CRM System In Healthcare Organization." International Journal of Computer Engineering & Sciences (IJCES) 1.2 (2011): 28-35.